Recent results on hyperon-nucleon interactions at BESIII

Jielei Zhang
(zhangjielei@ihep.ac.cn)

Henan University

Outline

- Motivation
- BEPCII and BESIII
- Study of $\Xi^0 n \to \Xi^- p$
  PRL 130, 251902 (2023)
- Study of $\Lambda N \to \Sigma^+ X$
  PRC 109, L052201 (2024)
- Study of $\Lambda p \to \Lambda p$ and $\bar{\Lambda} p \to \bar{\Lambda} p$
  PRL 132, 231902 (2024)
- Summary

Scattering experiments of particle beams bombarding target materials

1911

Ernest Rutherford

$\alpha + \mathrm{Au}$

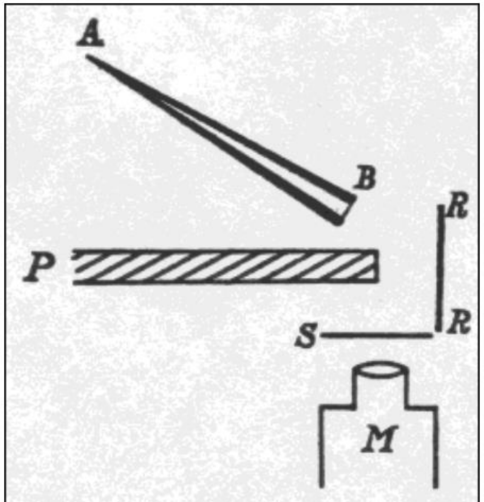

Fig. 1.

Nuclear structure model of atom

1919 $\alpha + \mathrm{N}$ → Observation of proton

1932 $\alpha + \mathrm{Be}$ → Observation of neutron

James Chadwick

Scattering experiments of particle beams bombarding target materials

1974

$p + \mathrm{Be} \rightarrow e^{+}e^{-}X$

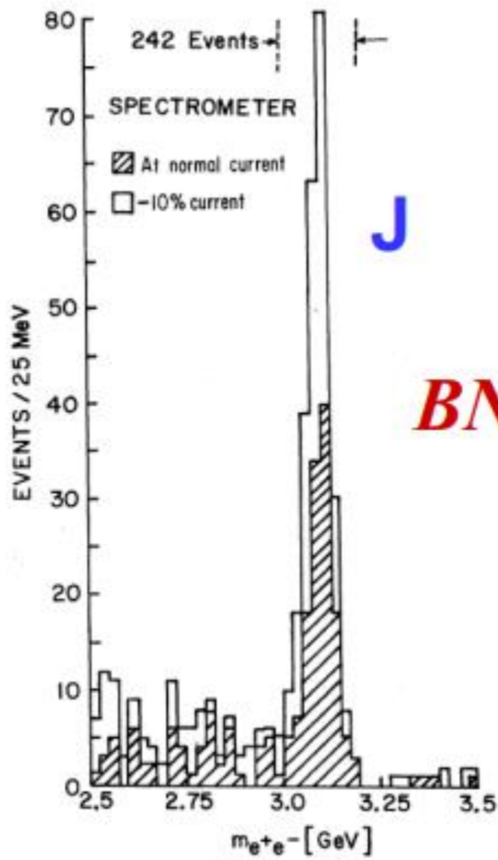

J.J. Aubert et al., PRL 33, 1404 (1974)

J

BNL

Discovery of the fourth type of quark:
Charm quark

"November Revolution in Physics"

Nobel Prize 1976

Scattering experiment must have **particle source**, target material, and detector.

Hyperon source

Baryon octet

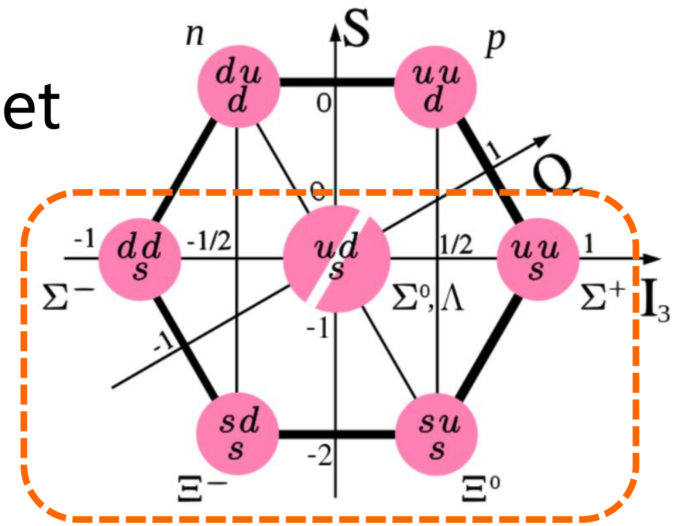

One of main goals of nuclear physics is to understand baryon-baryon interaction in a unified perspective

Limited by availability and short-lifetime of hyperon beams

- Hyperons are obtained by bombarding hydrogen bubble chamber or scintillating fiber target with K^-.

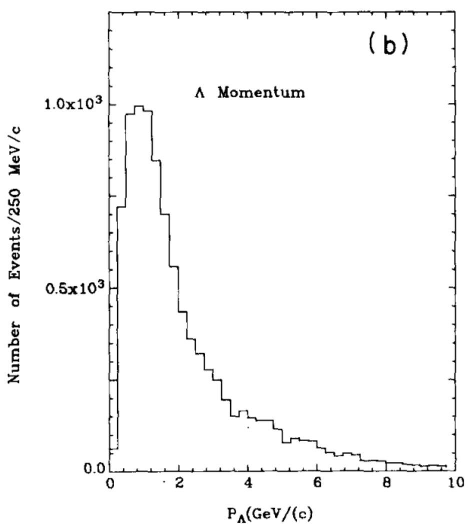

NPB 125, 29 (1977)

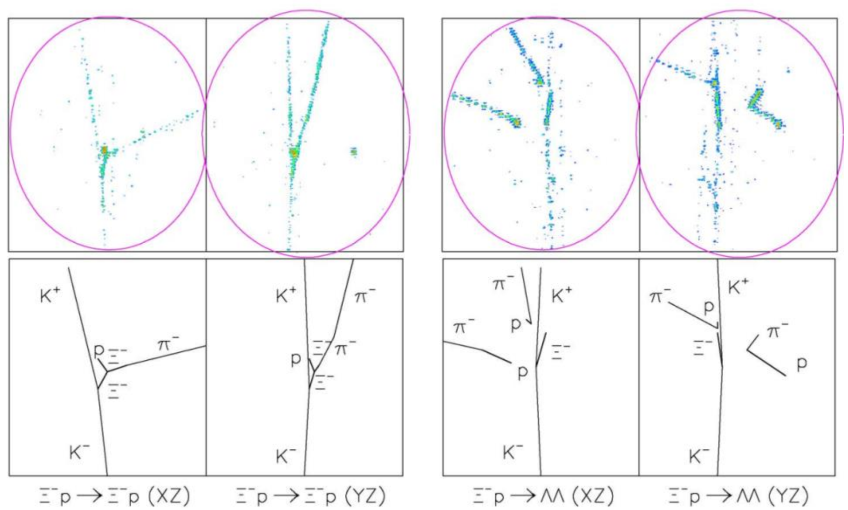

PLB 633, 214 (2006)

Hyperon source

- Hyperons are obtained by bombarding hydrogen bubble chamber or scintillating fiber target with K^-.
- Intensity of hyperon beams is low, experimental measurements are scarce and have large uncertainty.
- No anti-hyperon source.

Reaction	Number of events	
$\Lambda p \to \Lambda p$ (elastic)	584	(1)
$\Lambda p \to \Sigma^- p \pi^+$	132	(2)
$\Lambda p \to \Sigma^+ p \pi^-$	60	(3)
$\Lambda p \to \Lambda p \pi^+ \pi^-$	181	(4)
$\Lambda p \to \Sigma^0 p$	35	(5)
various $\Xi^0 p$ interactions	25	

PLB 38, 123 (1972)

reaction	events *	signature	cross-section events **	cross-section (mb)
$\Xi^0 + p \to \Xi^0 + p$	2	K, Λ	1	8
$\Xi^0 + p \to \Lambda + \Sigma^+$	6	Λ	4	24
$\Xi^0 + p \to \Sigma^0 + \Sigma^+$	1	Λ	1	6
$\Xi^0 + p \to \pi^+ + \Lambda + \Lambda$	1	K, Λ	1	6
$\Xi^0 + p \to \pi^0 + \Lambda + \Sigma^+$	1	Λ	1	6
$\Xi^0 + p \to \pi^+ + \Xi^- + p$	1	K or Λ	1	5
$\Xi^0 + p \to \pi^+ + \pi^+ + \Xi^- + n$	1	K, Λ	1	6
$\Xi^0 + p \to \Xi^- + p$	2	Λ	2	8
$\Xi^0 + p \to \Sigma^- + \Sigma^+$	1	K	1	4
$\Xi^0 + p \to \Sigma^- + K^0 + p$	1	K	1	4

PLB 32, 720 (1970)

Reaction	Momentum interval (GeV/c)	Number of events	σ (mb)
$\Lambda p \to$ all	0.5 → 1.0		25.8 ± 6.2
	1.0 → 1.5		31.3 ± 6.5
	1.5 → 2.0		42.8 ± 7.1
	2.0 → 2.5		37.5 ± 7.2
	2.5 → 3.0		34.1 ± 8.3
	3.0 → 4.0		41.8 ± 10.0
$\Lambda p \to \Lambda p$	0.5 → 1.0	20	22.2 ± 5.0
	1.0 → 1.5	21	12.9 ± 2.8
	1.5 → 2.0	37	22.0 ± 3.6
	2.0 → 2.5	28	16.1 ± 3.1
	2.5 → 3.0	12	11.0 ± 3.2
	3.0 → 4.0	13	12.5 ± 3.4
$\Lambda p \to \Sigma^0$	0.66 → 4.0	11	1.5 ± 0.5
$\Lambda p \to \Lambda p \pi^0$	0.88 → 4.0	29	4.1 ± 0.8
$\Lambda p \to \Lambda p \pi^+ \pi^-$	1.36 → 4.0	12	1.9 ± 0.6
$\Sigma^+ p \to \Sigma^+ p$	0.5 → 1.5	10	31.2 ± 10.1
	1.5 → 2.5	8	18.7 ± 6.6
	2.5 → 4.0	4	15.3 ± 7.8
$\Sigma^- p \to \Sigma^- p$	0.5 → 1.5	6	13.2 ± 4.7
	1.5 → 2.5	11	13.9 ± 4.1
	2.5 → 4.0	4	7.5 ± 3.8
$\Xi^- p \to \Xi^- p$	1.0 → 4.0	6	13 ± 6
$\Xi^0 p \to \Xi^0 p$	1.0 → 4.0	4	19 ± 10

NPB 125, 29 (1977)

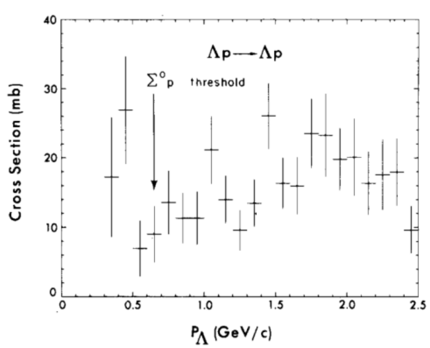

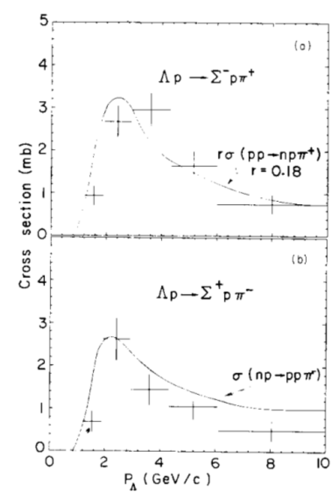

PLB 633, 214 (2006)

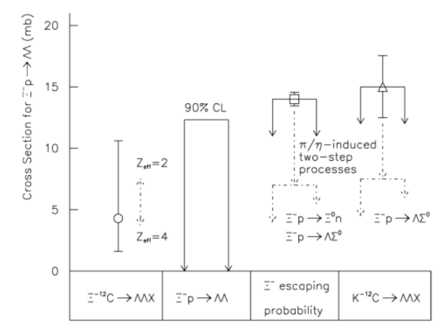

Theory of hyperon-nucleon (YN) interaction has large uncertainty due to lack of relevant measurements

PRC 105, 035203 (2022)

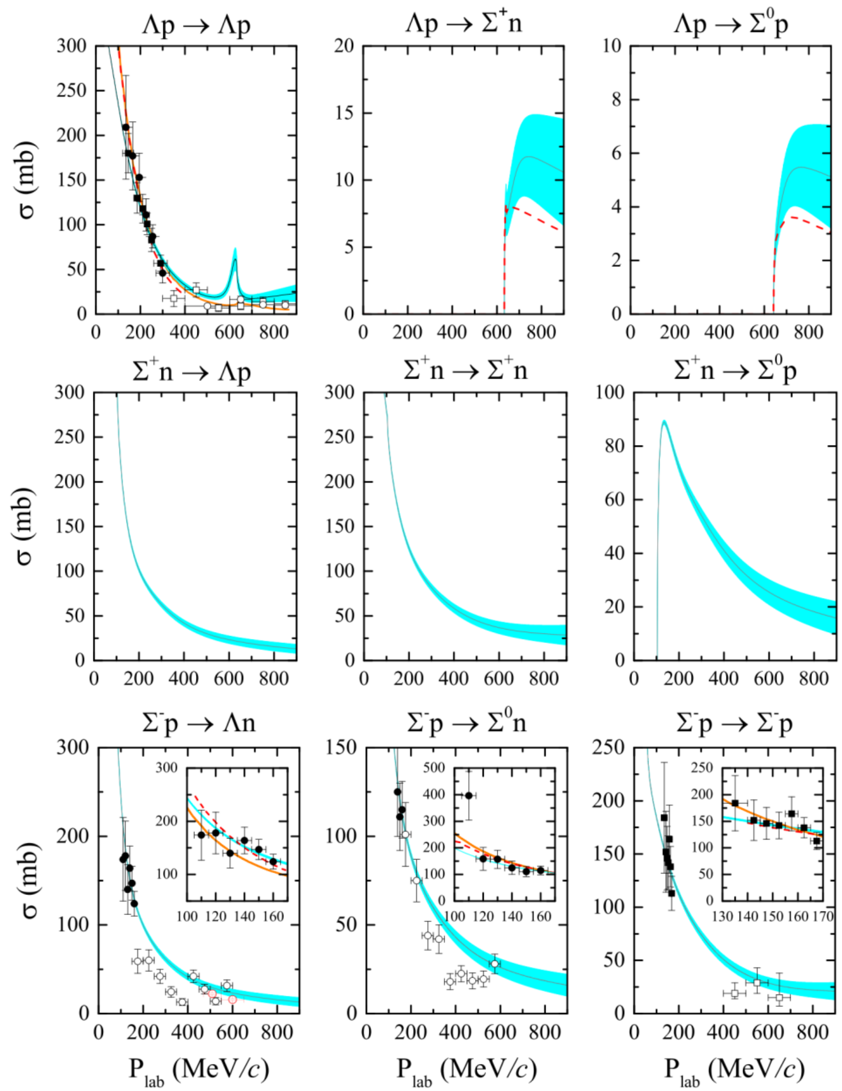

LO : H. Polinder, J.H., U.-G. Meißner, PLB 653 (2007) 29

NLO16: J.H., U.-G. Meißner, S. Petschauer, NPA 954 (2016) 273

NLO19: J.H., U.-G. Meißner, EPJA 55 (2019) 23

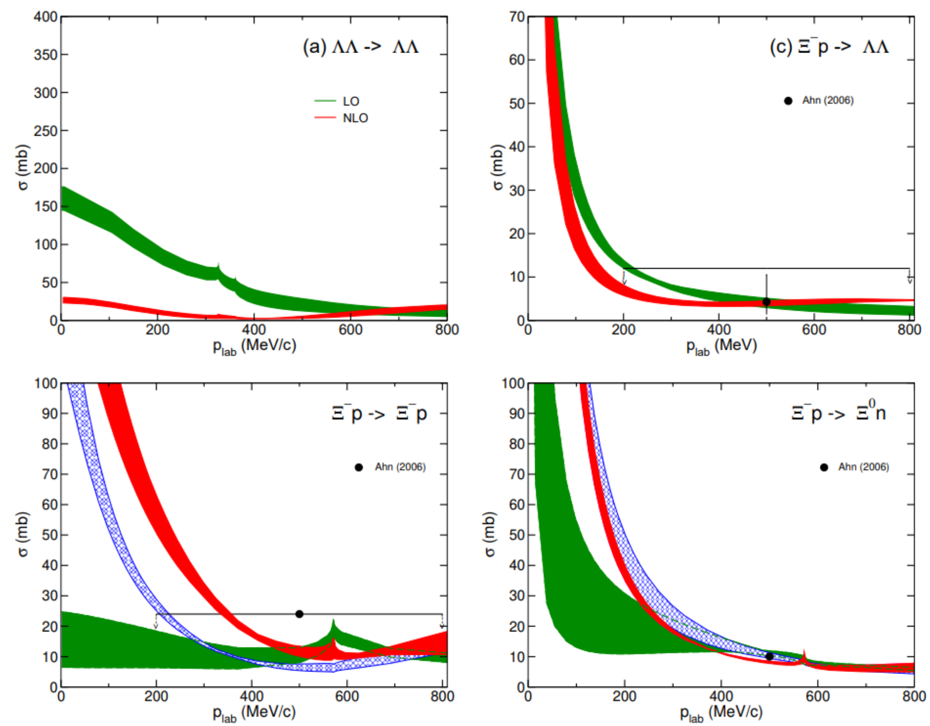

"Hyperon puzzle" of neutron stars

- Hyperons are believed to be appeared in inner core of neutron stars.

$$B_1 \rightarrow B_2 + l + \bar{\nu}_l,\ B_2 + l \rightarrow B_1 + \nu_l$$

$$n \rightarrow p + e^- + \bar{\nu}_e, p + e^- \rightarrow n + \nu_e \qquad \Sigma^- \rightarrow n + e^- + \bar{\nu}_e, n + e^- \rightarrow \Sigma^- + \nu_e$$

$$\Lambda \rightarrow p + e^- + \bar{\nu}_e, p + e^- \rightarrow \Lambda + \nu_e \qquad \Xi^- \rightarrow \Lambda + e^- + \bar{\nu}_e, \Lambda + e^- \rightarrow \Xi^- + \nu_e$$

- Appearance of hyperons softens equation of state, lead to maximum mass that neutron stars can sustain is less than mass of already-observed neutron stars.
- A repulsive force is introduced to stiffen equation of state in theory, such as a combination of ΛN and ΛNN interactions. Study of hyperon-nucleon interaction is crucial to solve "hyperon puzzle" of neutron stars.

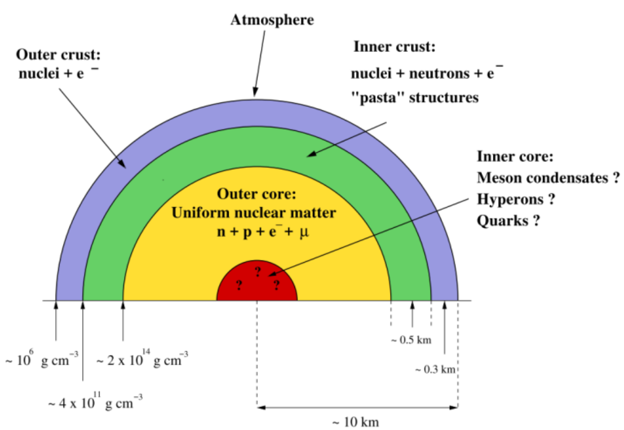

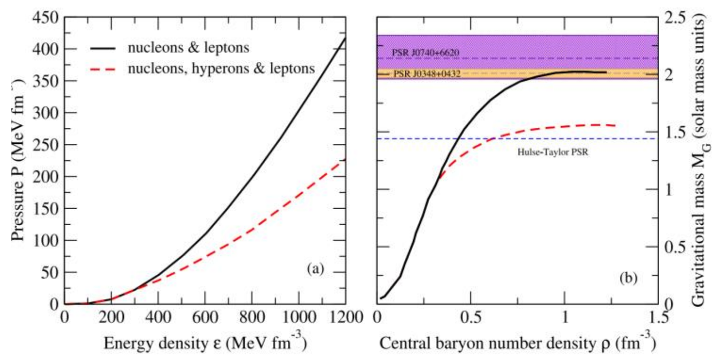

PPNP 112, 103770 (2020)

PRL 114, 092301 (2015)

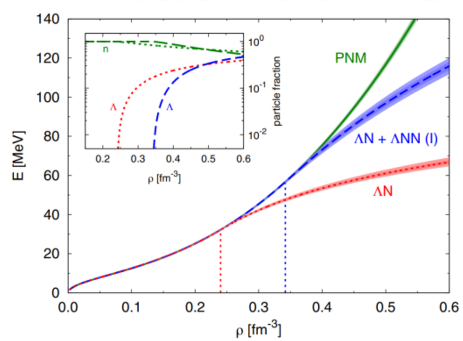

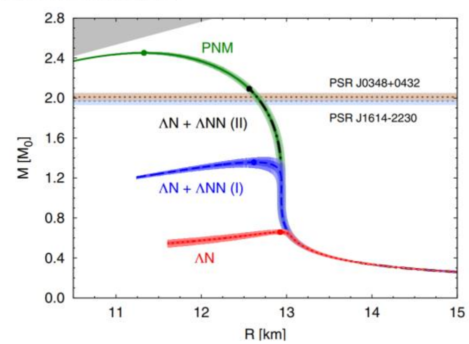

Some recent experimental results on hyperon-nucleon scattering

PHYSICAL REVIEW LETTERS **127**, 272303 (2021)

(CLAS Collaboration)

Improved Λp Elastic Scattering Cross Sections between 0.9 and 2.0 GeV/c as a Main Ingredient of the Neutron Star Equation of State

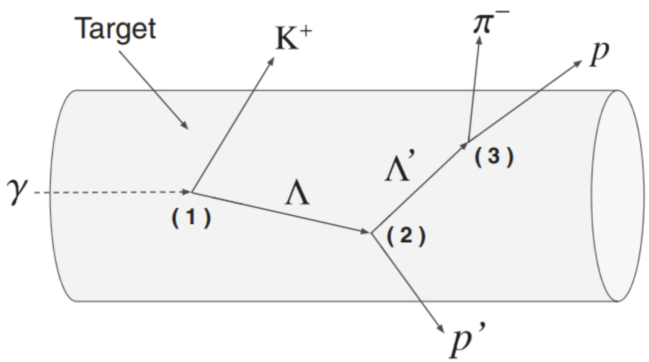

$$\sigma(p_\Lambda) = \frac{Y(p_\Lambda)}{A(p_\Lambda) \times \mathcal{L}(p_\Lambda) \times \Gamma}$$

$$\mathcal{L}(p_\Lambda) = \frac{N_A \times \rho_T \times l}{M} N_\Lambda(p_\Lambda)$$

$\Lambda p \rightarrow \Lambda p$

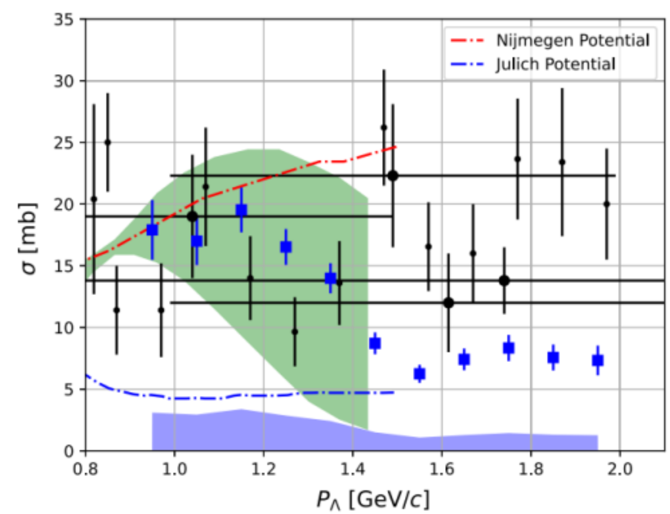

This is the first data on this reaction since the 1970s.

Some recent experimental results on hyperon-nucleon scattering

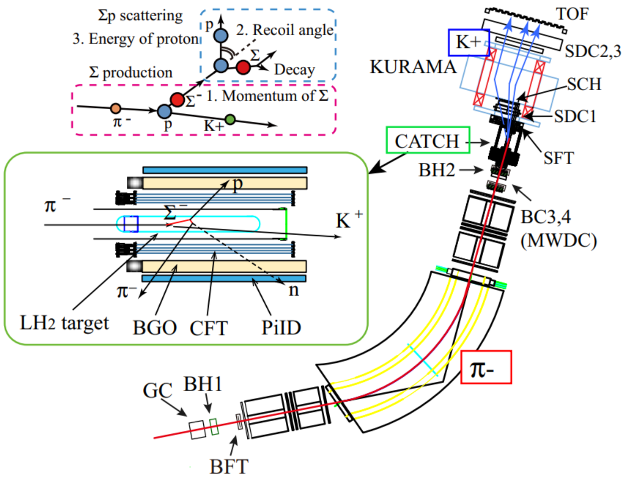

J-PARC E40 Collaboration

PRC 104, 045204 (2021)

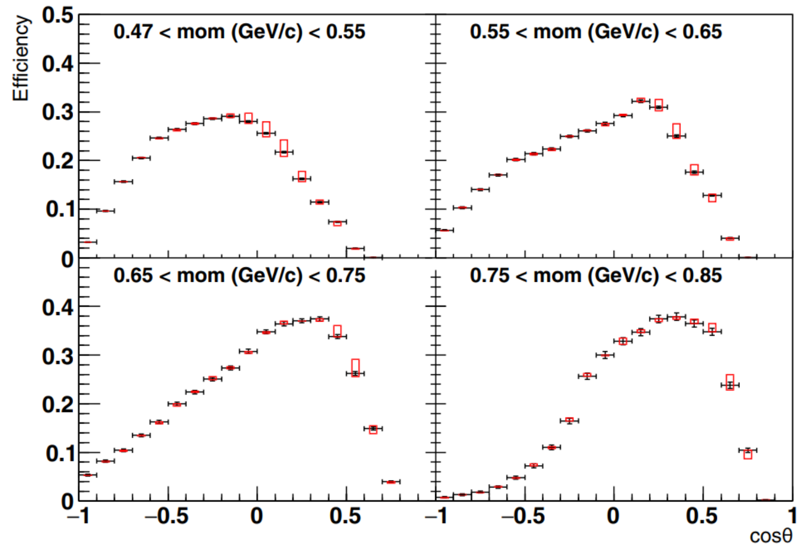

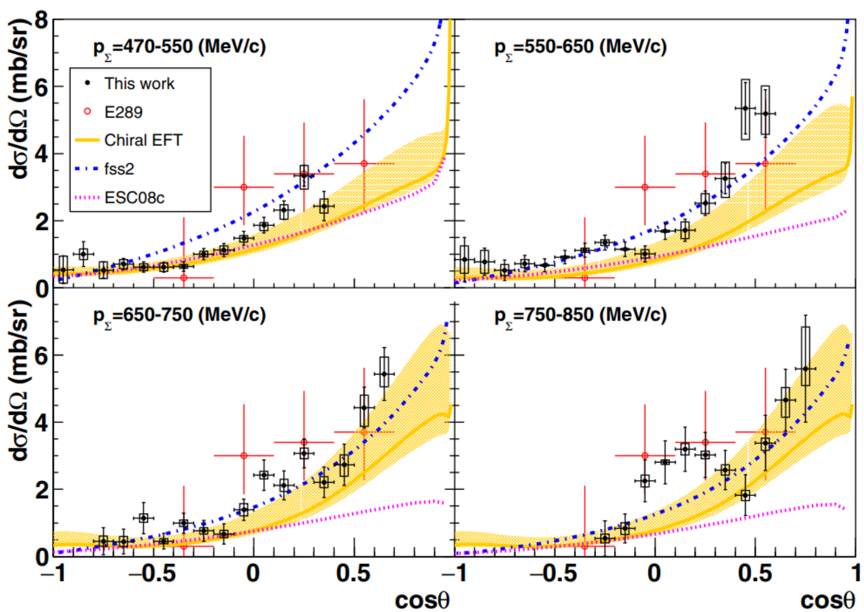

$$\Sigma^- p \rightarrow \Sigma^- p$$

Some recent experimental results on hyperon-nucleon scattering

J-PARC E40 Collaboration

PTEP 2022, 093D01 (2022)

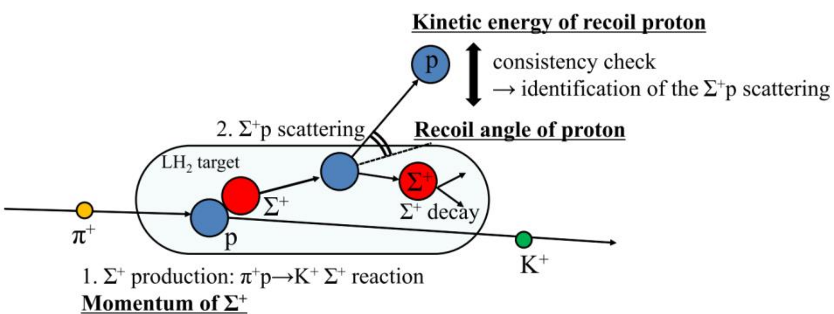

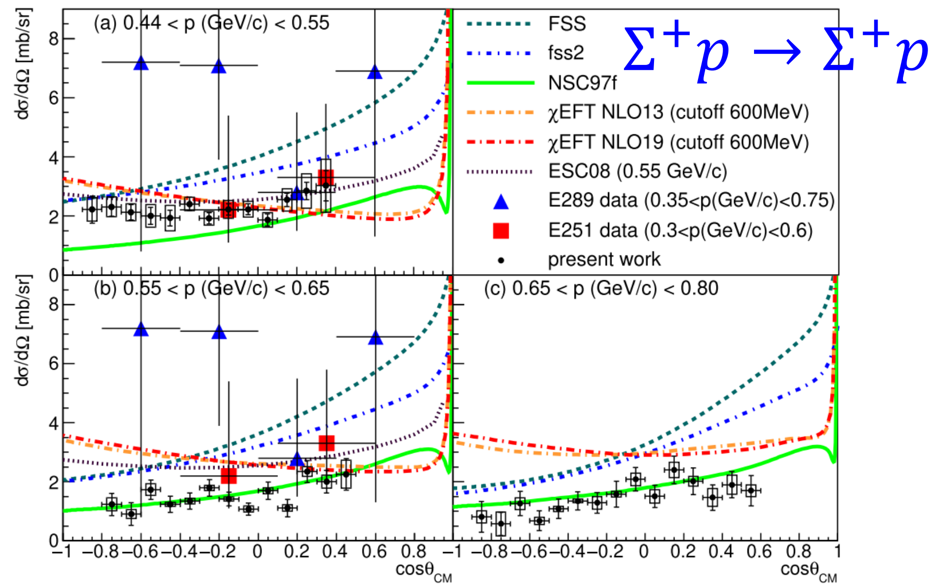

PRL 128, 072501 (2022)

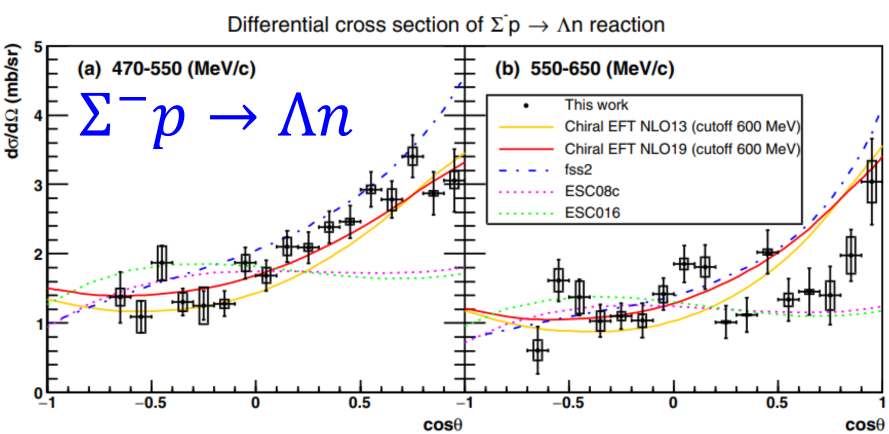

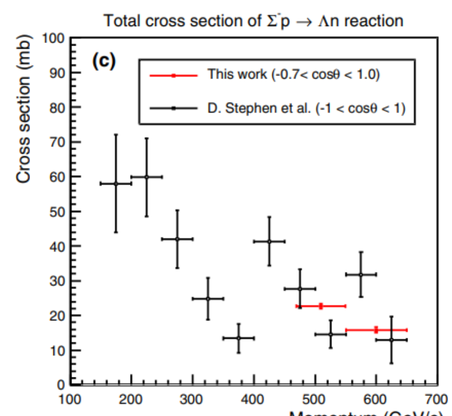

Beijing Electron Positron Collider II (BEPCII) and Beijing Spectrometer III (BESIII)

tau-charm energy region

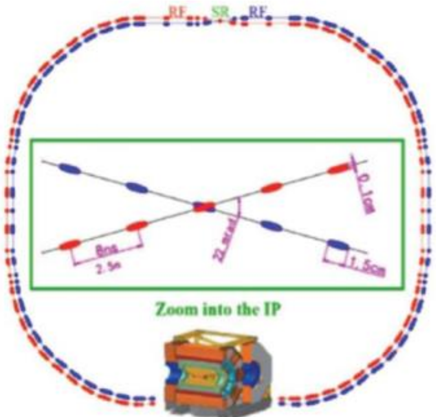

Storage ring

Linear accelerator

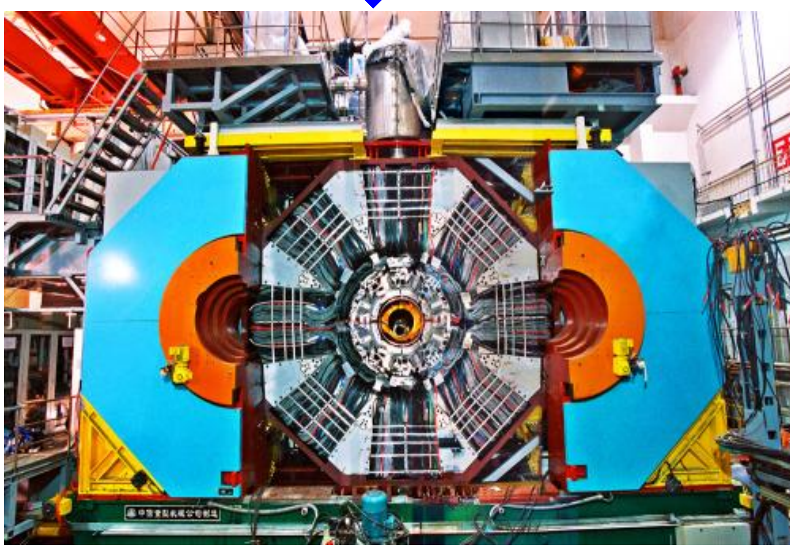

BESIII detector

BEPCII

BESIII detector

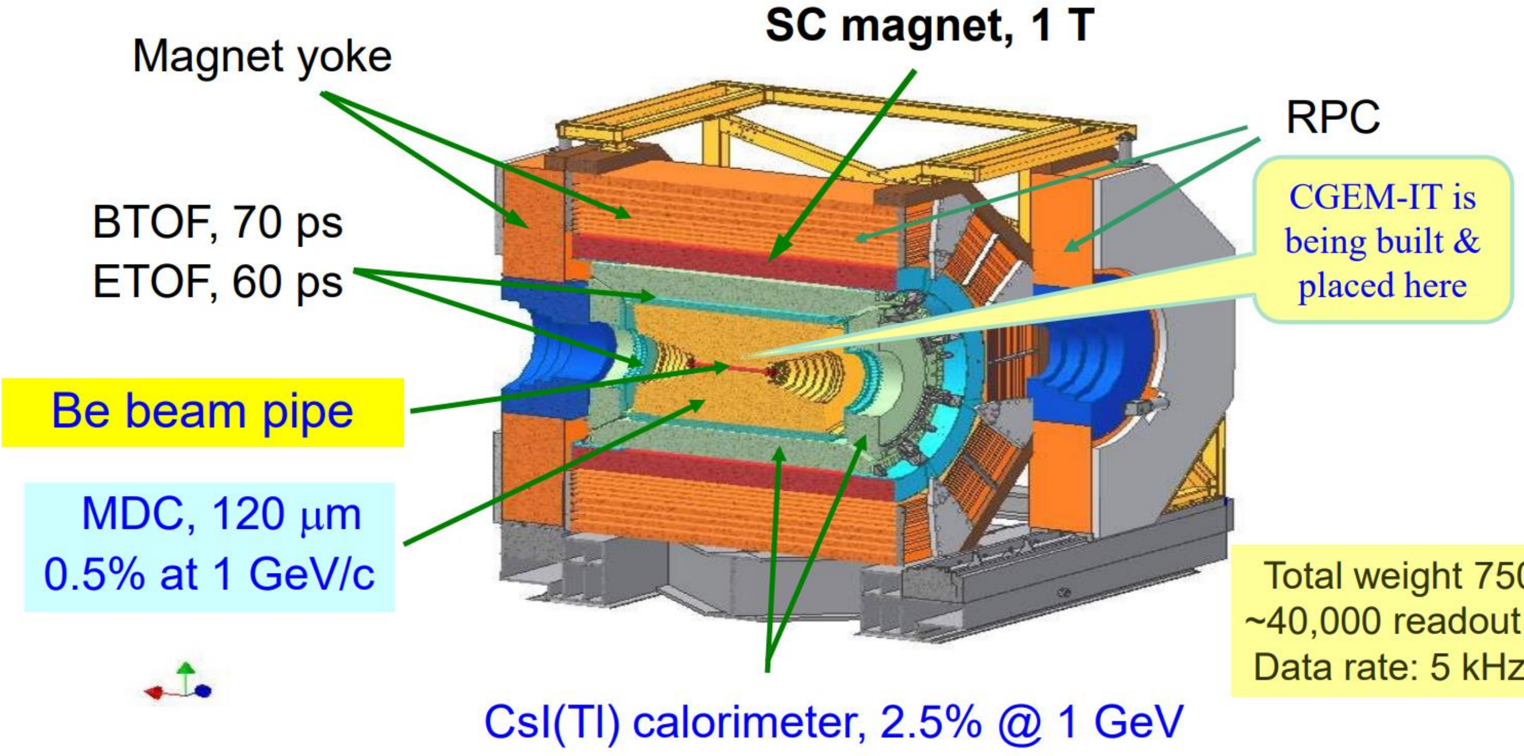

Total weight 750 tonnes,
~40,000 readout channels,
Data rate: 5 kHz, 50 Mb/s

Has been in full operation since 2008,
all subdetectors are in very good status!

BESIII data samples

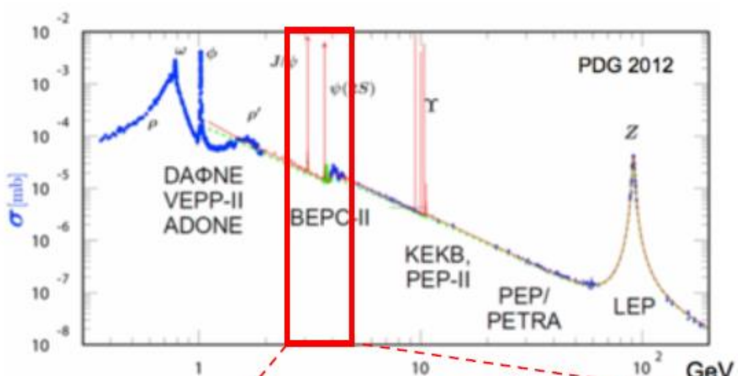

BESIII has collected the largest data samples of the J/ψ and $\psi(3686)$ in the world, and $> 20\ \mathrm{fb}^{-1}$ above $4.0\ \mathrm{GeV}$ in total.

10 billion J/ψ events

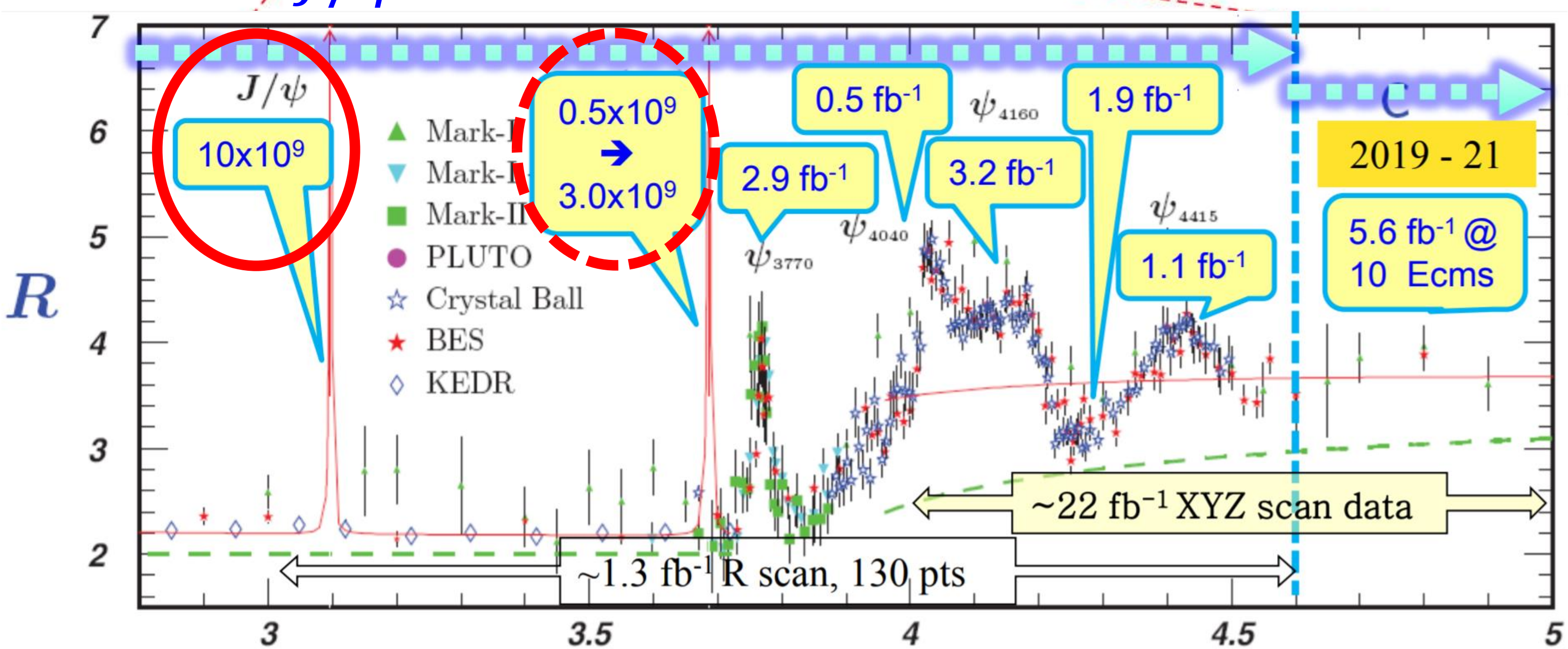

Experimental study on particle targeting at BESIII

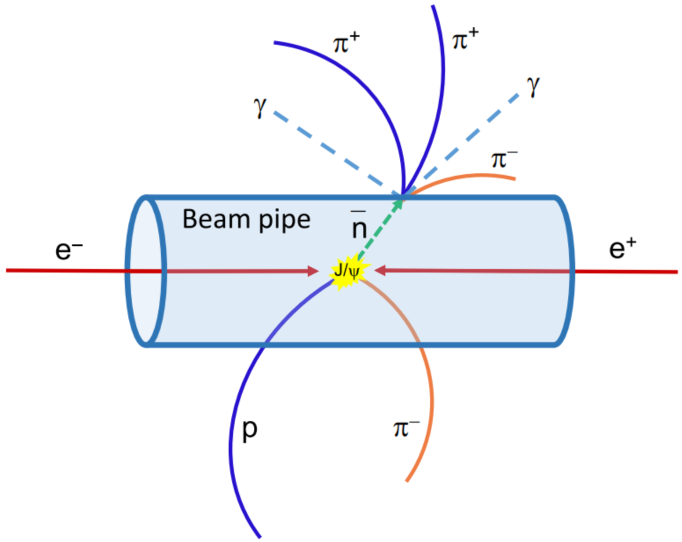

PRL 127, 012003 (2021)
CPC 48, 073003 (2024)

$\bar{n}p \rightarrow \pi^+\pi^+\pi^-\pi^0, \pi^0 \rightarrow \gamma\gamma$

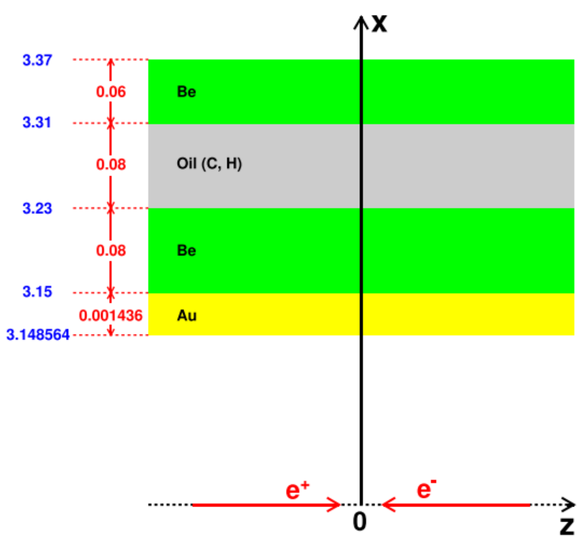

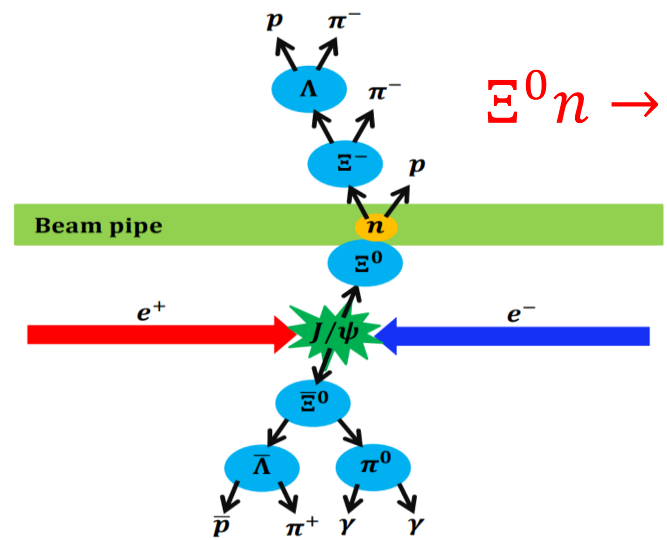

$\Xi^0 n \rightarrow \Xi^- p$

particle source: hyperon from J/ψ decays
target material: beam pipe
detector: BESIII detector

Recent results on hyperon-nucleon scattering at BESIII

- **First Study of Reaction $\Xi^0 n \to \Xi^- p$ Using Ξ^0-Nucleus Scattering at an Electron-Positron Collider**
  PRL 130, 251902 (2023)

- **First measurement of ΛN inelastic scattering with Λ from $e^+e^- \to J/\psi \to \Lambda\bar{\Lambda}$**
  PRC 109, L052201 (2024)

- **First Study of Antihyperon-Nucleon Scattering $\bar{\Lambda}p \to \bar{\Lambda}p$ and Measurement of $\Lambda p \to \Lambda p$ Cross Section**
  PRL 132, 231902 (2024)

Study of $\Xi^0 n \to \Xi^- p$

PRL 130, 251902 (2023)

Reaction chain :

$J/\psi \to \Xi^0\bar{\Xi}^0$, $\bar{\Xi}^0 \to \bar{\Lambda}\pi^0$, $\bar{\Lambda} \to \bar{p}\pi^+$, $\pi^0 \to \gamma\gamma$,
$\Xi^0 n \to \Xi^- p$, $\Xi^- \to \Lambda\pi^-$, $\Lambda \to p\pi^-$.

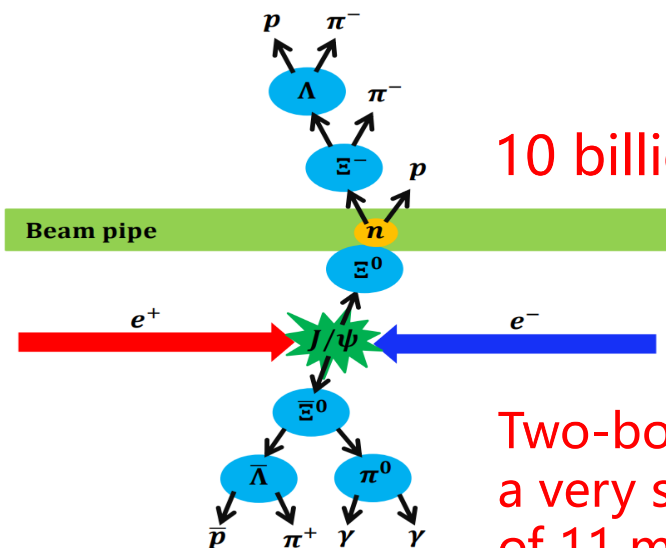

10 billion J/ψ data

Two-body decay, $P_{\Xi^0} \approx 0.818$ GeV$/c$, a very small horizontal crossing angle of 11 mrad for e^+ and e^- beams.

Analysis method :

Using $\bar{\Xi}^0$ to tag the event and requiring the recoiling mass in Ξ^0 region. Then reconstructing Ξ^- and p in the signal side.

Study of $\Xi^0 n \to \Xi^- p$

R_{xy} is distance from reconstructed $\Xi^- p$ vertex to z axis

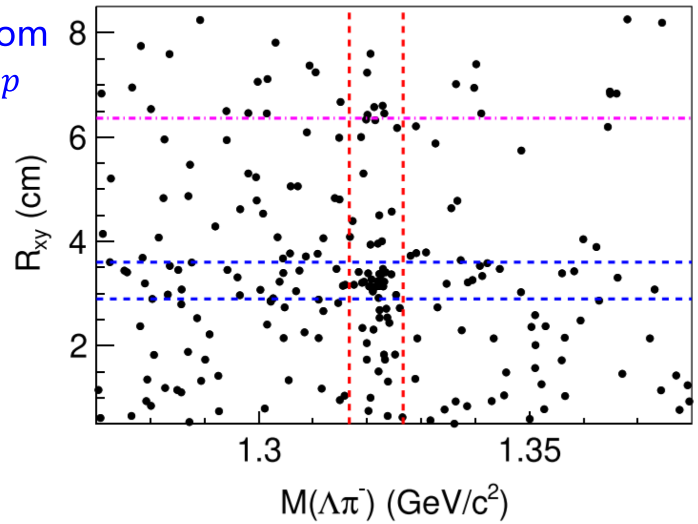

Inner wall of MDC

Beam pipe

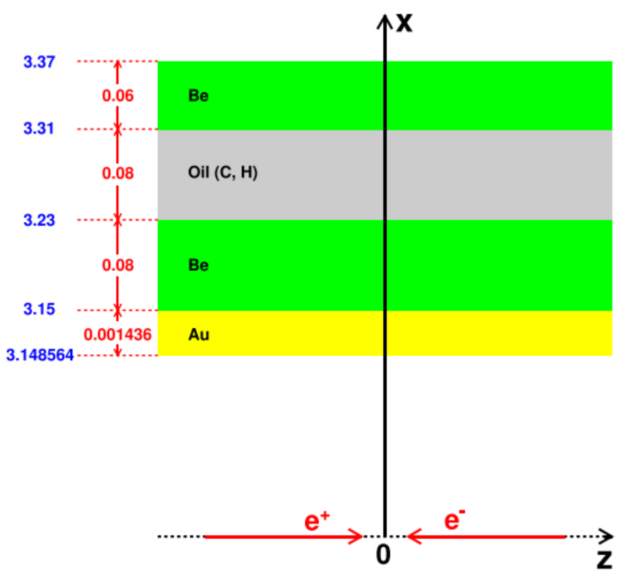

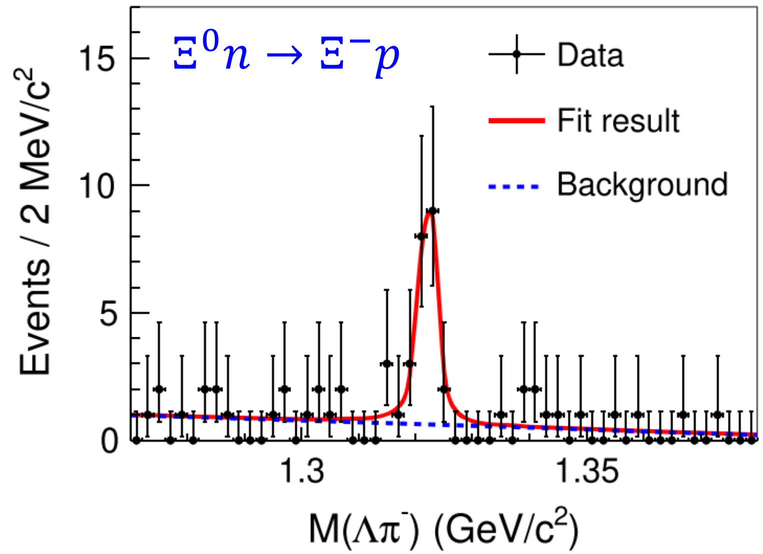

$N = 22.9 \pm 5.5$

$S = 7.1\sigma$

Cross section of $\Xi^0 + {}^9\text{Be} \rightarrow \Xi^- + p + {}^8\text{Be}$

$$\sigma(\Xi^0 + {}^9\text{Be} \rightarrow \Xi^- + p + {}^8\text{Be}) = \frac{N^{\text{sig}}}{\epsilon \mathcal{B} \mathcal{L}_{\text{eff}}}$$

$$\mathcal{L}_{\text{eff}} = \frac{N_{J/\psi}\mathcal{B}_{J/\psi}}{2+\frac{2}{3}\alpha} \int_a^b \int_0^\pi (1+\alpha\cos^2\theta) e^{-\frac{x}{\sin\theta\beta\gamma L}} N(x) C(x) d\theta dx$$

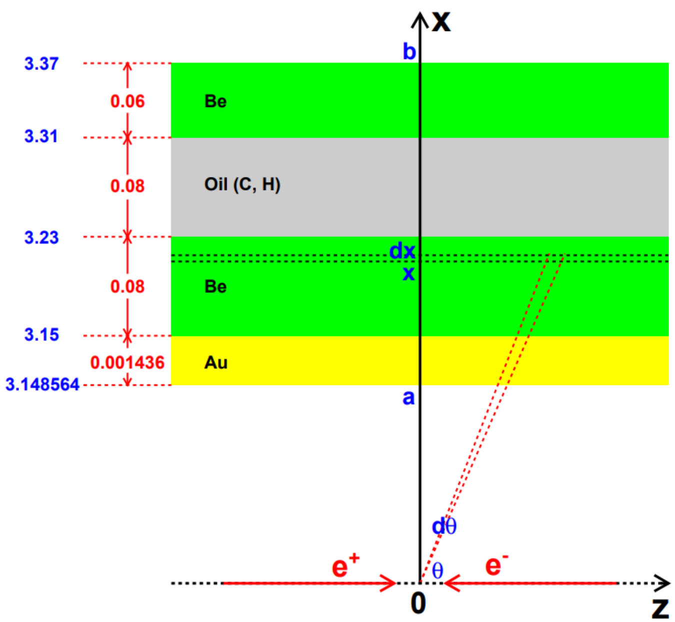

Parameter	Result
N^{sig}	22.9 ± 5.5
ϵ	1.873%
$\mathcal{B}$	$(40.114 \pm 0.444)\%$ [53]
$N_{J/\psi}$	$(1.0087 \pm 0.0044) \times 10^{10}$ [46]
$\mathcal{B}_{J/\psi}$	$(0.117 \pm 0.004)\%$ [53]
α	0.514 ± 0.016 [56]
L	(8.69 ± 0.27) cm [53]
E_{beam}	1.5485 GeV
m_{Ξ^0}	$(1.31486 \pm 0.00020)\ \text{GeV}/c^2$ [53]
a	3.148564 cm [45]
b	3.37 cm [45]
$N(x)$	$\begin{cases} 5.91 \times 10^{22}\ \text{cm}^{-3}, & 3.148564 \le x \le 3.15\ \text{cm} \\ 1.24 \times 10^{23}\ \text{cm}^{-3}, & 3.15 < x \le 3.23\ \text{cm} \\ 3.45 \times 10^{22}\ \text{cm}^{-3}, & 3.23 < x \le 3.31\ \text{cm} \\ 1.24 \times 10^{23}\ \text{cm}^{-3}, & 3.31 < x \le 3.37\ \text{cm} \end{cases}$
$C(x)$	$\begin{cases} 8.437(23.6), & 3.148564 \le x \le 3.15\ \text{cm} \\ 1.000(1.00), & 3.15 < x \le 3.23\ \text{cm} \\ 1.090(1.20), & 3.23 < x \le 3.31\ \text{cm} \\ 1.000(1.00), & 3.31 < x \le 3.37\ \text{cm} \end{cases}$

$\sigma \propto A^{\alpha'}$

α' is about $\frac{2}{3}\sim 1$

pure surface process assumption
(proportional to number of neutrons)

Study of $\Xi^0 n \to \Xi^- p$

The measured cross section of the reaction process $\Xi^0 + {}^9\mathrm{Be} \to \Xi^- + p + {}^8\mathrm{Be}$ is $\sigma(\Xi^0 + {}^9\mathrm{Be} \to \Xi^- + p + {}^8\mathrm{Be}) = (22.1 \pm 5.3_{\mathrm{stat}} \pm 4.5_{\mathrm{sys}})$ mb at $P_{\Xi^0} \approx 0.818$ GeV/c.

If we take the effective number of reaction neutrons in ${}^9\mathrm{Be}$ nucleus as 3, the cross section of $\Xi^0 n \to \Xi^- p$ for single neutron is determined to be $\sigma(\Xi^0 n \to \Xi^- p) = (7.4 \pm 1.8_{\mathrm{stat}} \pm 1.5_{\mathrm{sys}})$ mb, consistent with theoretical predictions.

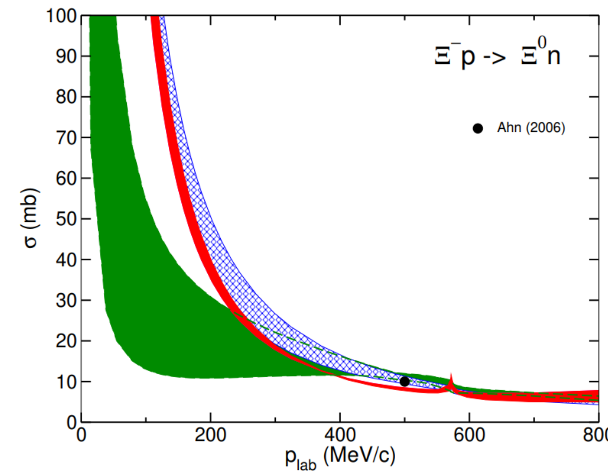

LO : H. Polinder, J.H., U.-G. Meißner, PLB 653 (2007) 29
NLO16: J.H., U.-G. Meißner, S. Petschauer, NPA 954 (2016) 273
NLO19: J.H., U.-G. Meißner, EPJA 55 (2019) 23

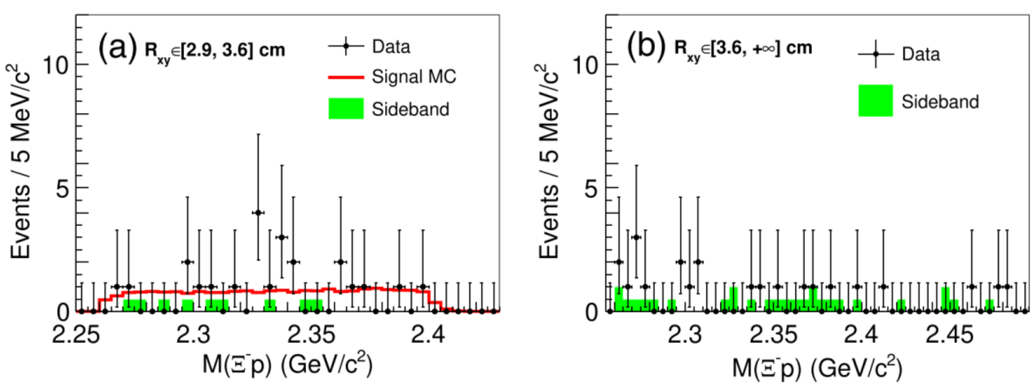

No significant H-dibaryon signals are seen

This work is the first study of hyperon-nucleon interaction in electron-positron collisions, and opens up a new direction for such research.

Study of $\Lambda N \to \Sigma^+ X$

PRC 109, L052201 (2024)

Reaction chain :

$J/\psi \to \Lambda\bar{\Lambda}$, $\bar{\Lambda} \to \bar{p}\pi^+$, $\Lambda + N(\text{nucleus}) \to \Sigma^+ + X(\text{anything})$, $\Sigma^+ \to p\pi^0$, $\pi^0 \to \gamma\gamma$.

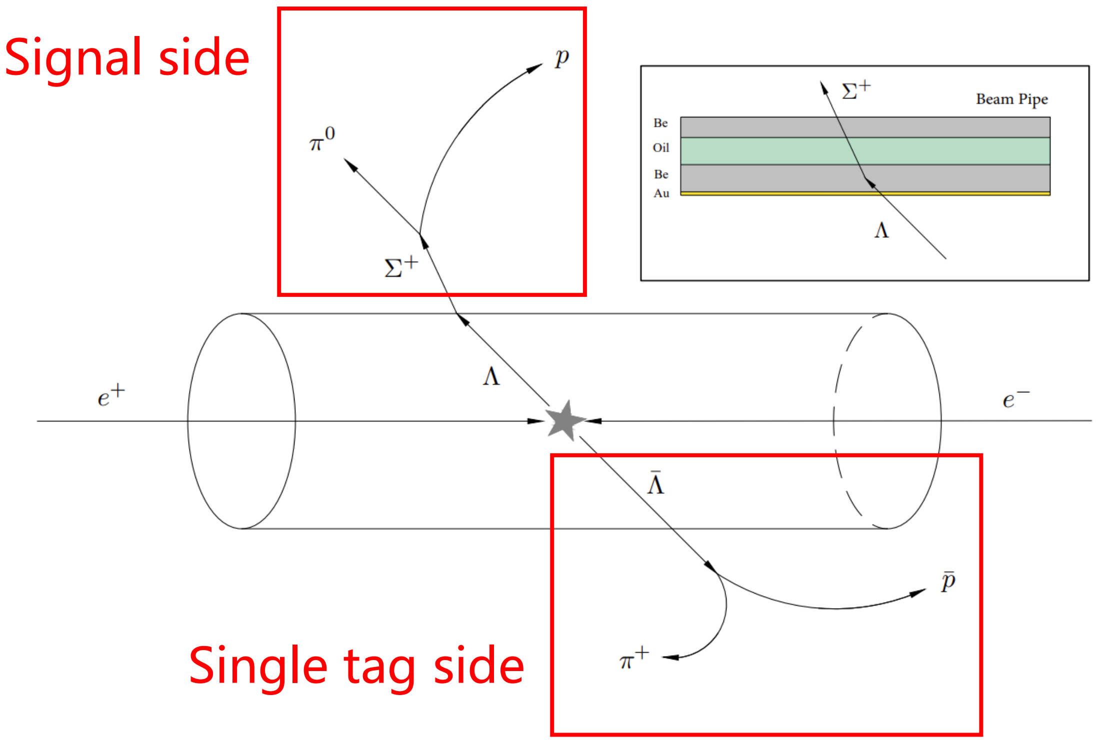

Two-body decay,
$P_\Lambda \approx 1.074~\mathrm{GeV}/c$,
a very small horizontal crossing angle of 11 mrad for e^+ and e^- beams, resulting in a small range of $0.017~\mathrm{GeV}/c$ above and below $1.074~\mathrm{GeV}/c$ for P_Λ.

Study of $\Lambda N \to \Sigma^+ X$

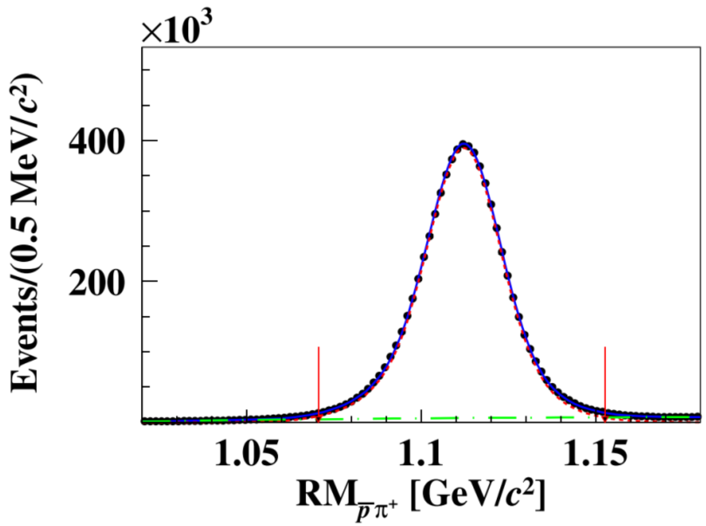

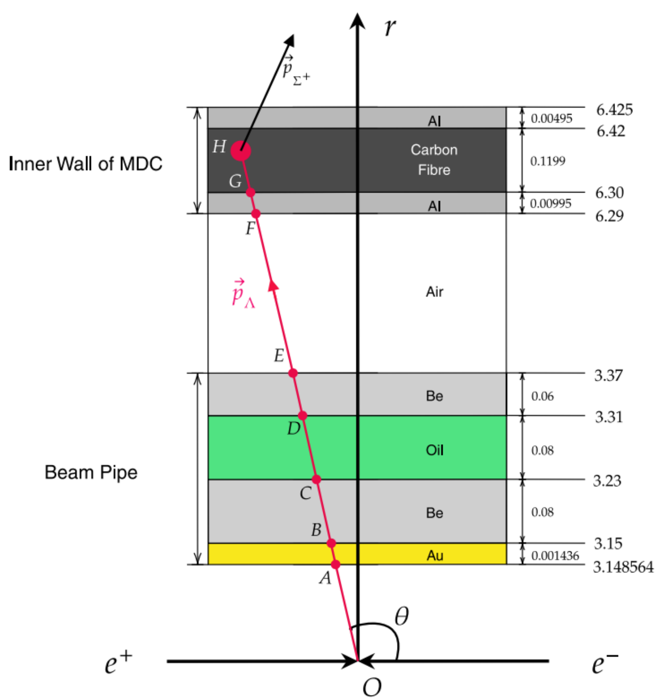

$N_{\mathrm{ST}} = 7207565 \pm 3741$

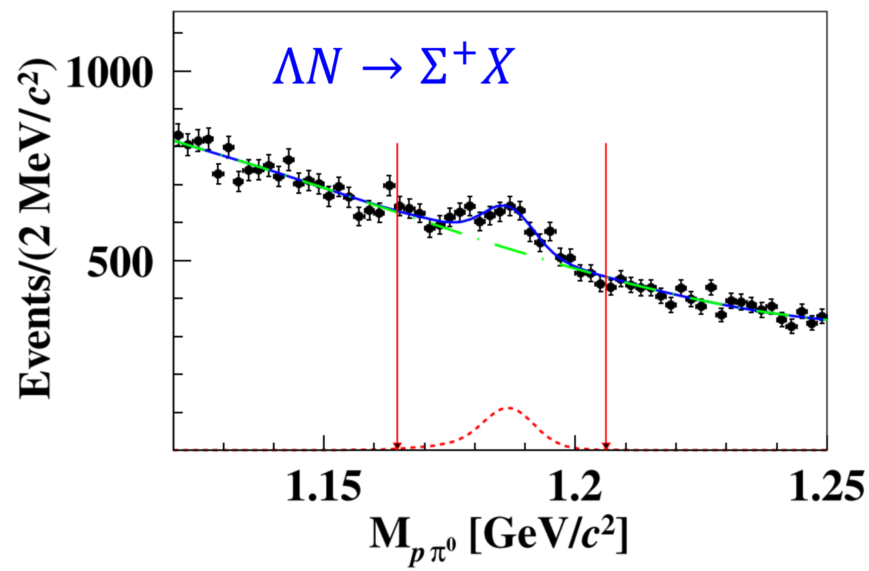

$N_{\mathrm{DT}} = 795 \pm 101$

The reaction position can not be determined. These signal events mainly come from the reaction with beam pipe and inner wall of MDC.

Cross section of $\Lambda + {}^9\text{Be} \to \Sigma^+ + X$

$$\sigma(\Lambda + {}^9\text{Be} \to \Sigma^+ + X) = \frac{N_{\text{DT}}}{\epsilon_{\text{sig}} \mathcal{L}_\Lambda} \frac{1}{\mathcal{B}(\Sigma^+ \to p\pi^0)}$$

$$\mathcal{L}_\Lambda = N_{\text{ST}} \frac{N_A}{N_{\text{ST}}^{\text{MC}}} \sum_j^7 \sum_i^{N_{\text{ST}}^{\text{MC}}} \frac{\rho_T^j l^{ij}}{M^j} \mathcal{R}_\sigma^j$$

path length of incident Λ of i_{th} event inside j_{th} layer

pure surface process assumption (proportional to number of protons)

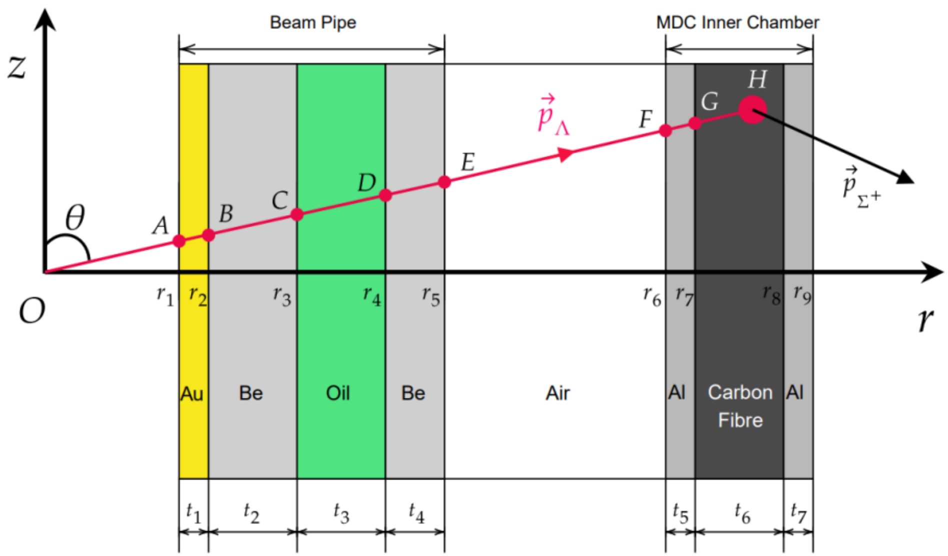

Parameter	Value
N_{DT}	795 ± 101
ϵ_{sig}	24.32%
$\mathcal{L}_\Lambda$	$(17.00 \pm 0.01) \times 10^{28}\ \text{cm}^{-2}$
$\mathcal{B}(\Sigma^+ \to p\pi^0)$	$(51.57 \pm 0.30)\%$

Study of $\Lambda N \to \Sigma^+ X$

The measured cross section of the reaction process $\Lambda + {}^9\mathrm{Be} \to \Sigma^+ + X$ is $\sigma(\Lambda + {}^9\mathrm{Be} \to \Sigma^+ + X) = (37.3 \pm 4.7_{\mathrm{stat}} \pm 3.5_{\mathrm{sys}})$ mb at $P_\Lambda \approx 1.074$ GeV$/c$. This work represents the first attempt to investigate Λ-nucleus interaction at an e^+e^- collider.

If taking the effective number of reaction protons in ${}^9\mathrm{Be}$ nucleus as 1.93, the cross section of $\Lambda p \to \Sigma^+ X$ for single proton is determined to be $\sigma(\Lambda p \to \Sigma^+ X) = (19.3 \pm 2.4_{\mathrm{stat}} \pm 1.8_{\mathrm{sys}})$ mb.

$\sigma(\Lambda p \to \Sigma^+ n)$ is twice of $\sigma(\Lambda p \to \Sigma^0 p)$

NPB 125, 29 (1977)

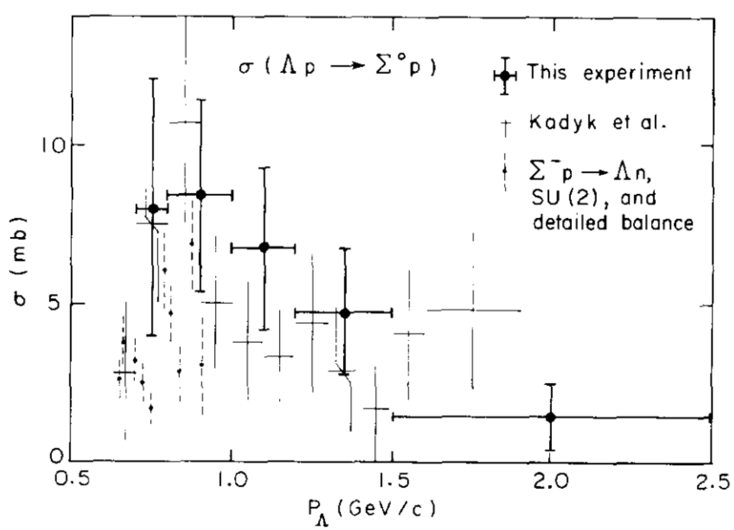

PRC 105, 035203 (2022)

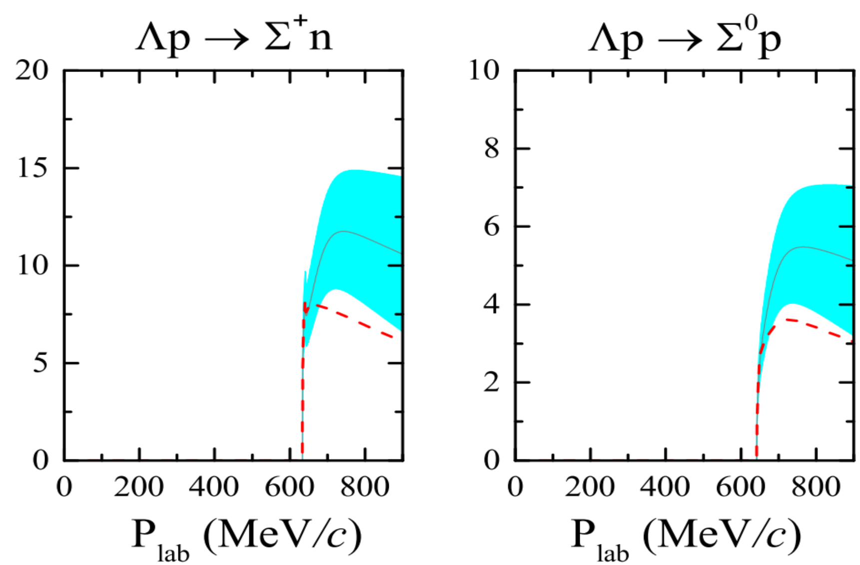

Study of $\Lambda p \to \Lambda p$ and $\bar{\Lambda} p \to \bar{\Lambda} p$

PRL 132, 231902 (2024)

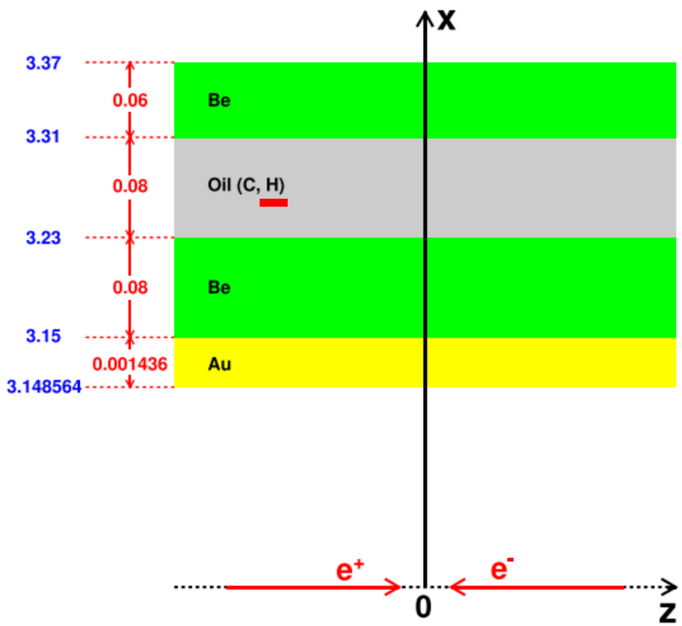

Taking the hydrogen in the cooling oil of the beam pipe as target material, the information on the hyperon-proton scattering can be extracted directly.

Two-body decay, $P_{\Lambda/\bar{\Lambda}} \approx 1.074\ \mathrm{GeV}/c$

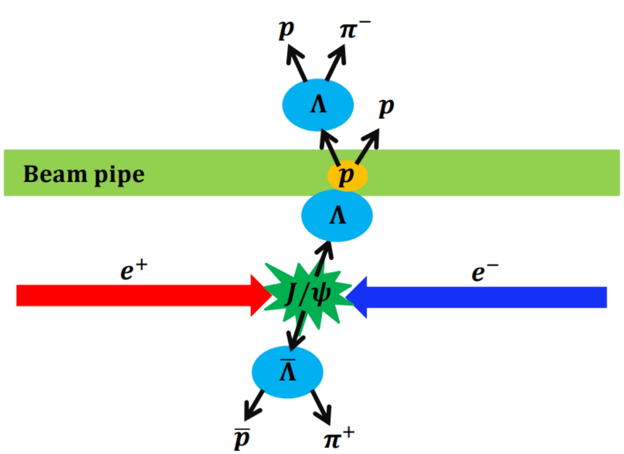

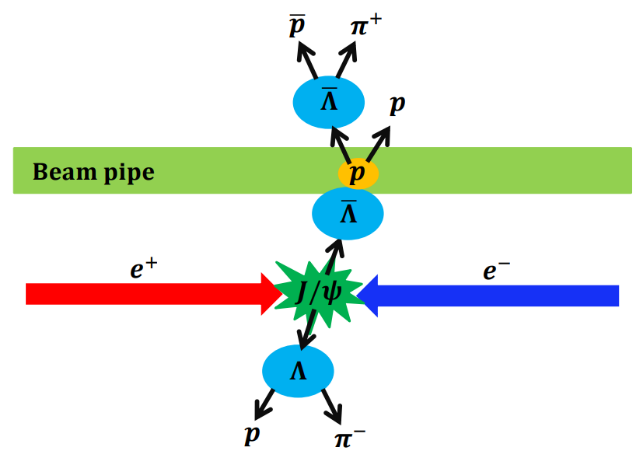

Study of $\Lambda p \to \Lambda p$ and $\bar{\Lambda} p \to \bar{\Lambda} p$

The center-of-mass energy for the incident $\Lambda/\bar{\Lambda}$ and a static p is about 2.243 GeV/c^2.

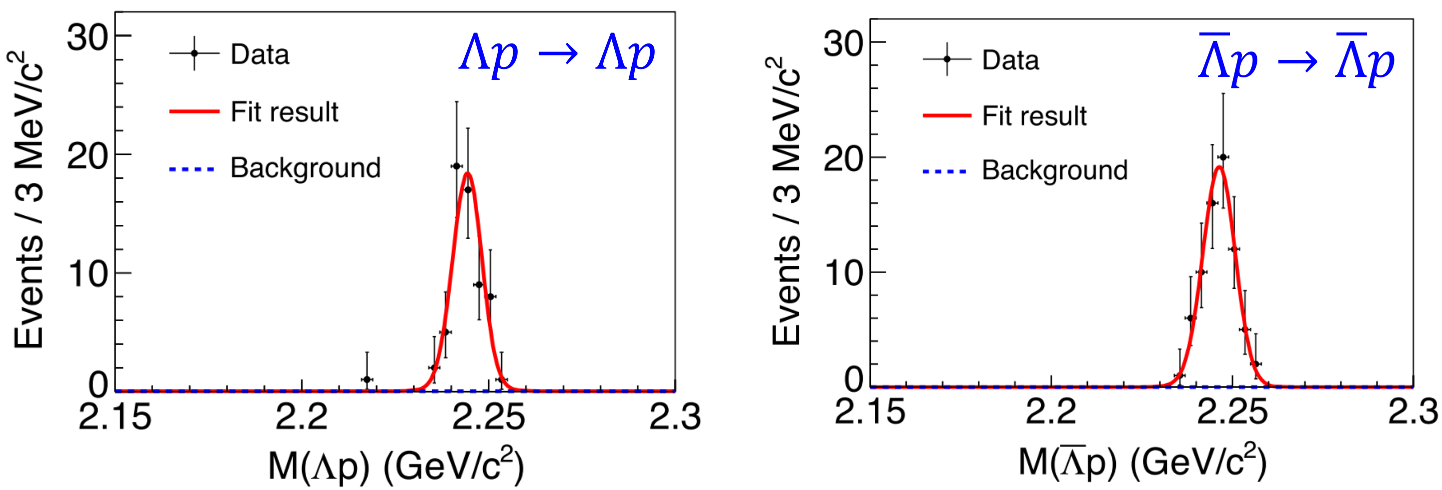

$$\sigma(\Lambda p \to \Lambda p/\bar{\Lambda} p \to \bar{\Lambda} p) = \frac{N^{\text{sig}}_{\Lambda p/\bar{\Lambda} p}}{\epsilon_{\Lambda p/\bar{\Lambda} p} \mathcal{B} \mathcal{L}_{\text{eff}}}$$

$$\left(\frac{d\sigma}{d\Omega}\right)_i = \frac{N_i^{\text{sig}}}{\epsilon_i \mathcal{B} \mathcal{L}_{\text{eff}} \Delta\Omega}$$

$$\mathcal{L}_{\text{eff}} = \frac{N_{J/\psi} \mathcal{B}_{J/\psi}}{2 + \frac{2}{3}\alpha} \int_a^b \int_0^\pi (1 + \alpha \cos^2\theta) e^{-\frac{x}{\sin\theta \beta\gamma L}} N_H \, \mathrm{d}\theta \mathrm{d}x$$

Study of $\Lambda p \rightarrow \Lambda p$ and $\bar{\Lambda} p \rightarrow \bar{\Lambda} p$

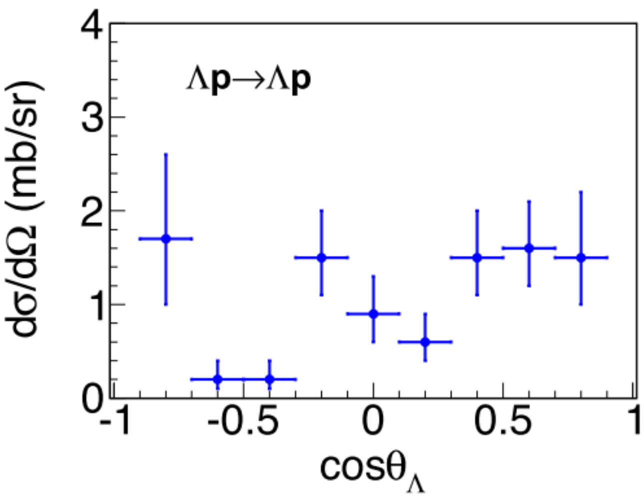

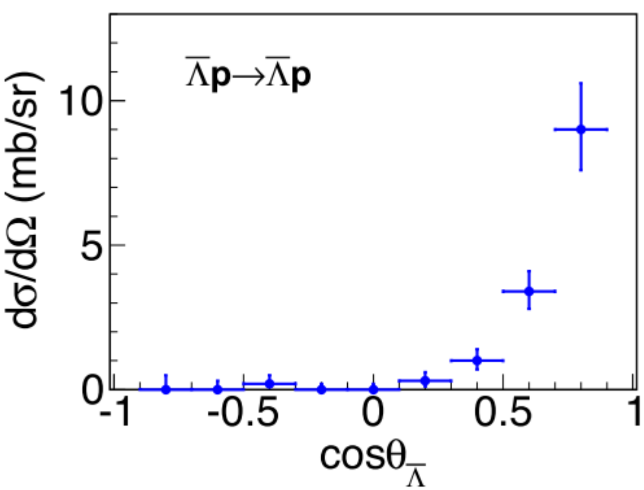

$\cos\theta_{\Lambda/\bar{\Lambda}}$	N_i^{sig}	ϵ_i (%)	$(d\sigma/d\Omega)$ (mb/sr)
$[-0.9, -0.7]$	$(5.0^{+2.6}_{-1.9}, 0.0^{+1.1}_{-0.0})$	(6.94,4.93)	$(1.7^{+0.9}_{-0.7}, 0.0^{+0.5}_{-0.0})$
$(-0.7, -0.5]$	$(1.0^{+1.4}_{-0.7}, 0.0^{+1.1}_{-0.0})$	(14.13,10.44)	$(0.2^{+0.2}_{-0.1}, 0.0^{+0.3}_{-0.0})$
$(-0.5, -0.3]$	$(1.0^{+1.4}_{-0.7}, 1.0^{+1.4}_{-0.7})$	(17.32,13.27)	$(0.2^{+0.2}_{-0.1}, 0.2^{+0.3}_{-0.1})$
$(-0.3, -0.1]$	$(11.0^{+3.7}_{-3.0}, 0.0^{+1.1}_{-0.0})$	(17.74,14.66)	$(1.5^{+0.5}_{-0.4}, 0.0^{+0.2}_{-0.0})$
$(-0.1, 0.1]$	$(6.9^{+3.0}_{-2.3}, 0.0^{+1.1}_{-0.0})$	(19.11,15.79)	$(0.9^{+0.4}_{-0.3}, 0.0^{+0.2}_{-0.0})$
$(0.1, 0.3]$	$(5.0^{+2.6}_{-1.9}, 2.0^{+1.8}_{-1.1})$	(19.53,16.82)	$(0.6^{+0.3}_{-0.2}, 0.3^{+0.3}_{-0.2})$
$(0.3, 0.5]$	$(12.0^{+3.8}_{-3.1}, 7.0^{+3.0}_{-2.3})$	(19.21,17.68)	$(1.5^{+0.5}_{-0.4}, 1.0^{+0.4}_{-0.3})$
$(0.5, 0.7]$	$(13.0^{+3.9}_{-3.3}, 25.0^{+5.3}_{-4.7})$	(19.71,17.60)	$(1.6^{+0.5}_{-0.4}, 3.4^{+0.7}_{-0.6})$
$(0.7, 0.9]$	$(6.0^{+2.8}_{-2.1}, 37.0^{+6.4}_{-5.8})$	(9.80,9.93)	$(1.5^{+0.7}_{-0.5}, 9.0^{+1.6}_{-1.4})$

Cross sections in $-0.9 \leq \cos\theta_{\Lambda/\bar{\Lambda}} \leq 0.9$ are measured to be
$\sigma(\Lambda p \rightarrow \Lambda p) = (12.2 \pm 1.6_{\text{stat}} \pm 1.1_{\text{sys}})$ mb and
$\sigma(\bar{\Lambda} p \rightarrow \bar{\Lambda} p) = (17.5 \pm 2.1_{\text{stat}} \pm 1.6_{\text{stat}})$ mb

Total cross sections are determined to be
$\sigma_t(\Lambda p \rightarrow \Lambda p) = (14.2 \pm 1.8_{\text{stat}} \pm 1.3_{\text{sys}})$ mb and
$\sigma_t(\bar{\Lambda} p \rightarrow \bar{\Lambda} p) = (27.4 \pm 3.2_{\text{stat}} \pm 2.5_{\text{sys}})$ mb

Study of $\Lambda p \to \Lambda p$ and $\bar{\Lambda} p \to \bar{\Lambda} p$

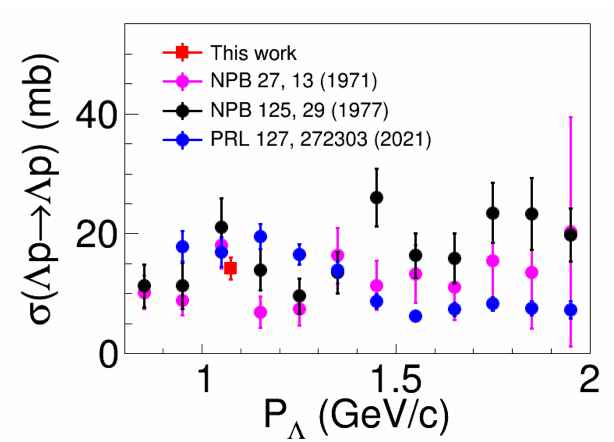

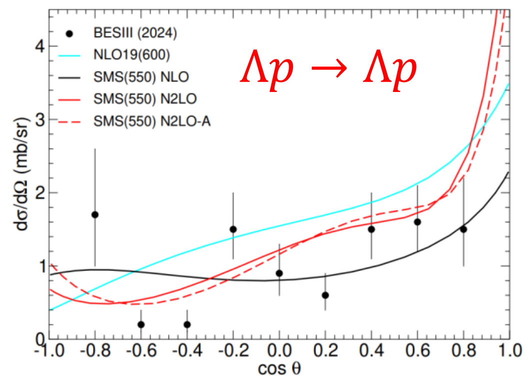

J. Haidenbauer and U. G. Meiβner, EPJA 60, 119 (2024)

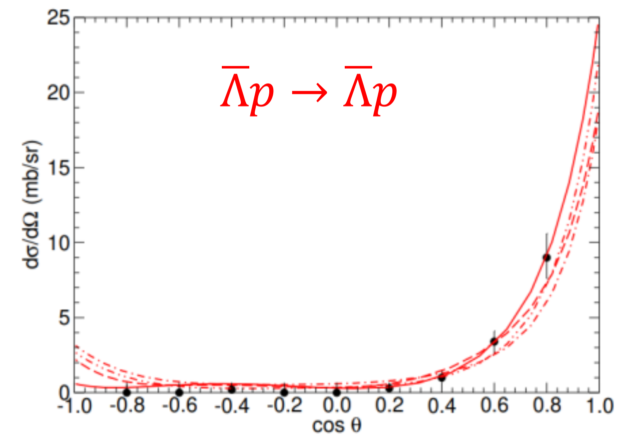

Fig. 1 Differential cross section for $p\bar{\Lambda}$ scattering at $p_{lab} = 1.074 \pm 0.017$ GeV [59]. The curves are predictions by the $\Lambda\bar{\Lambda}$ interactions I-IV, see Ref. [35], at 1.05 GeV/c.

Phys. Rev. 112, 1303 (1958)

"black sphere" scattering

$$\frac{d\sigma}{d\Omega} = k^2 R^4 \left[\frac{J_1(2kR\sin(\theta/2))}{2kR\sin(\theta/2)} \right]^2,$$

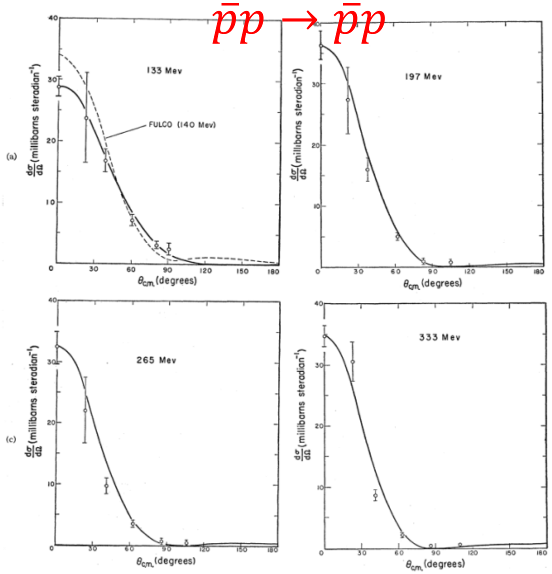

strong absorption/annihilation

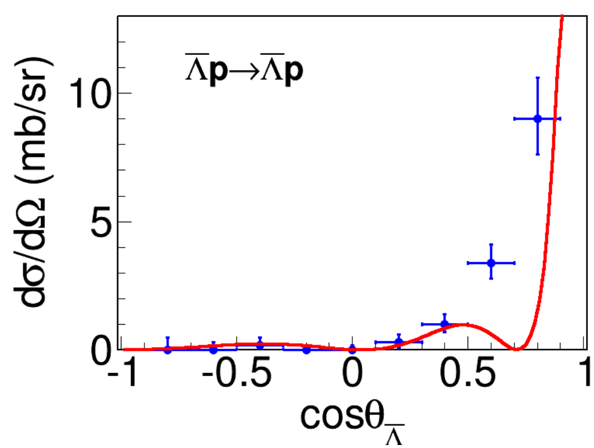

Table 2 $\Lambda\bar{\Lambda}$ scattering lengths (in fm) in the $^1S_0$ and $^3S_1$ partial waves of the employed $\Lambda\bar{\Lambda}$ potentials [41,43]. The spin-averaged value by the ALICE Collaboration is from an analysis of the $\Lambda\bar{\Lambda}$ correlation function measured in Pb-Pb collisions [21]

potential	$a(^1S_0)$	$a(^3S_1)$
I	0.32 − i0.52	0.74 − i0.56
II	0.67 − i1.14	0.66 − i0.37
III	1.42 − i1.15	1.00 − i0.44
IV	1.56 − i1.40	0.98 − i0.65
ALICE	(0.90 ± 0.16) − i(0.40 ± 0.18)	

Some ongoing researches on hyperon-nucleon scattering at BESIII

- $\Sigma^+ n \to \Lambda p$, $\Sigma^+ n \to \Sigma^0 p$
- $\Xi^0 n \to \Lambda\Lambda$, $\Xi^- p \to \Lambda\Lambda$
- $\Sigma^+ p \to \Sigma^+ p$, $\bar{\Sigma}^- p \to \bar{\Sigma}^- p$
- $\Xi^- p \to \Xi^- p$, $\bar{\Xi}^+ p \to \bar{\Xi}^+ p$

……

More results will come out soon !!!

Summary

1. Using a novel method, hyperon-nucleon scattering can also be measured at BESIII now.

- $\Xi^0 n \to \Xi^- p$
- $\Lambda N \to \Sigma^+ X$
- $\Lambda p \to \Lambda p$
- $\bar{\Lambda} p \to \bar{\Lambda} p$

2. This is the first study of hyperon-nucleon scattering in electron-positron collisions, and opens up a new direction for such research. Especially, antihyperon-nucleon scattering is studied for the first time.

3. With more statistics in future super tau-charm facilities, the momentum-dependent cross section or differential cross section distributions can be studied based on the hyperons from multibody decays of J/ψ or other charmonia.

Thanks for your attention!